JOURNAL OF MATERIALS SCIENCE 23 (1988) 3258–3262

Fabrication of perovskite $Pb(Fe_{2/3}W_{1/3})_x(Fe_{1/2}Nb_{1/2})_{0.9-x}Ti_{0.1}O_3$ by double calcination process

GUNG-FU CHEN, SHEN-LI FU
Department of Electrical Engineering, National Cheng Kung University, Tainan, Taiwan

Perovskite, $Pb(Fe_{2/3}W_{1/3})_x(Fe_{1/2}Nb_{1/2})_{0.9-x}Ti_{0.1}O_3$ (abbreviated as $PFW_xPFN_{0.9-x}PT_{0.1}$ where PFW = $3PbO–Fe_2O_3–WO_3$, PFN = $4PbO–Fe_2O_3–Nb_2O_3$ and PT = $PbO–TiO_2$), can be fabricated by the so-called double calcination process. The process is to first partially calcine PFW, PFN and PT separately and then calcine the mixture of PFW, PFN and PT. A bulk density of at least 90% can be achieved with a sintering temperature of 900 to 930° C. The higher the molar proportion of PFW is, the lower the sintering temperature of $PFW_xPFN_{0.9-x}PT_{0.1}$ will be. This system shows a high dielectric constant (32 000) and a low loss tangent (1%). The effects of processing temperature on the sinterability and dielectric properties of $PFW_xPFN_{0.9-x}PT_{0.1}$ are also given.

1. Introduction

The demand for multilayer ceramic chip capacitors (MLCs) is growing rapidly to meet the development of surface-mount devices (SMDs) and the continuing miniaturization of integrated electronic circuits. Niobate-containing relaxors [1], e.g. $Pb(Mg_{1/2}Nb_{1/2})O_3$-based and $Pb(Fe_{1/2}Nb_{1/2})O_3$-based, have proved to be promising candidate dielectrics for MLCs due to their high dielectric constant, broad maximum and low firing temperature. However, it is difficult to produce the perovskite phase without the appearance of a pyrochlore phase.

Swartz and Shrout [2] presented a novel fabrication technique to eliminate the intermediate pyrochlore phase from lead magnesium niobate (PMN), but the reaction temperature of $MgNb_2O_6$ was the somewhat higher one of 1000° C. Lejeune and Biolot [3] derived monophase ceramics from PMN-based relaxors with a conventional ceramic process apart from the addition of 6 to 8% PbO after the calcining step. With the help of PbO, the firing temperature of PMN-based relaxors was reduced to the lower level of 900 to 1000° C.

In this work, a double calcination process was derived to prepare perovskite, $PFW_xPFN_{0.9-x}PT_{0.1}$; PFW = $3PbO–Fe_2O_3–WO_3$), PFN (= $4PbO–Fe_2O_3–Nb_2O_3$) and PT (= $PbO–TiO_2$) were first partially calcined at 600, 640 and 640° C, respectively. An intermediate phase was observed after the first calcination. The second calcination was conducted at temperature between 670 and 800° C to transform the intermediate phase into perovskite. This double calcination process does not possess the disadvantage of being time-consuming with problems in reproducibility and the control of PbO stoichiometry, as found in the conventional repeated calcination process.

2. Experimental procedure

2.1. Materials

The double calcination process was a conventional ceramic process apart from the two stages of calcination. Three batches of reagent-grade oxides $PbO–Fe_2O_3–WO_3$, $PbO–Fe_2O_3–Nb_2O_5$ and $PbO–TiO_2$ were first weighed with molar ratios of 3 : 1 : 1, 4 : 1 : 1 and 1 : 1, respectively. Each batch of weighed oxides was ball-milled in acetone for 8 h. After drying, calcining and grinding, partially calcined PFW, PFN and PT were obtained and then weighed according to the formulation of $PFW_xPFN_{0.9-x}PT_{0.1}$ and ball-milled in acetone for another 8 h. The second calcination was then carried out at 670 to 800° C.

Fabrication of $PFW_{0.41}PFN_{0.49}PT_{0.1}$ by a conventional ceramic process, i.e. direct mixing of all the constituent oxides, was also conducted to clarify the advantages of the double calcination process. The calcining conditions used in this work are listed in Table I. For the calcination conditions of Case 2, perovskite PFW, PFN and PT were preformed during the first calcination at 750° C, 700/900° C (repeatedly calcining at 700 and 900° C) and 750° C, respectively. Single-phase $PFW_xPFN_{0.9-x}PT_{0.1}$ was obtained by calcining the mixture of perovskite PFW, PFN and PT at 850° C. Case 2 is established to test the effect of an intermediate phase on the sinterability of $PFW_xPFN_{0.9-x}PT_{0.1}$.

2.2. Preparation of samples

Calcined slugs were pulverized with an agate mortar for a few hours. Ground powders were mixed with 5 wt % distilled water and uniaxially cold-pressed in a steel die of 1.27 cm diameter into a disc form. The pressing pressures was 20 kg cm^{-2}. Six stacked discs sprinkled with the same powder were fired in a closed

0022–2461/88 $03.00 + .12

TABLE I Calcining conditions used in this work

Conditions		1st calcination (°C)			2nd calcination (°C)
		$3PbO-Fe_2O_3-WO_3$	$4PbO-Fe_2O_3-Nb_2O_5$	$PbO-TiO_2$	$PFW_{0.41}PFN_{0.49}PT_{0.1}$
Case 1	No. 1	600	640	640	670
	No. 2	600	640	640	700
	No. 3	600	640	640	730
	No. 4	600	640	640	750
	No. 5	600	640	640	800
Case 2	No. 6	750	700/900	750	850
Case 3	No. 7	–	–	–	850

alumina crucible to minimize PbO vaporization. The soaking times of all the firing processes in this work were fixed at 2 h.

2.3. Measurements

Dielectric properties were measured using 1 mm thick discs with silver electrodes fired on both sides. The dielectric constant and loss tangent were derived from an HP4192A LF impedance analyser at 1 kHz with 1 V r.m.s.

The concentration of the perovskite phase was deduced from Cu$K\alpha$ X-ray diffraction (XRD) patterns according to the formula

$$\%(\text{pero.}) = \frac{I_{\text{pero.}}}{I_{\text{pero.}} + I_{\text{others}}} \times 100 \qquad (1)$$

where $I_{\text{pero.}}$ denote the maximum intensity of the perovskite diffraction peaks. I_{others} is the sum of the maximum intensities of non-perovskite phase peaks involving PbO, Fe_2O_3, $Pb_2Fe_2O_5$, pyrochlore phase etc.

3. Results and discussion

3.1. Dielectric properties of $PFW_xPFN_{0.9-x}PT_{0.1}$ prepared with conventional ceramic process (Case 3 of Table I)

The result of X-ray diffraction of $PFW_xPFN_{0.9-x}PT_{0.1}$ sintered at 970°C for 2 h is shown in Fig. 1. This composition was calcined at 850° C once only. Unfortunately, only 20% perovskite phase was obtained. Moreover, there were 76% parasitic $Pb_3Nb_4O_{13}$ pyrochlore phase and 4% unreacted Fe_2O_3. It is clear that nucleation of the perovskite phase was blocked by the stable pyrochlore phase. The linear shrinkage, dielectric constant and theoretical density of $PFW_xPFN_{0.9-x}PT_{0.1}$ fired at 970° C were 11%, 200 and 62.5%, respectively. The poor sinterability of $PFW_{0.41}PFN_{0.49}PT_{0.1}$ is ascribed to the high melting point (1225° C) [4] of the $Pb_3Nb_4O_{13}$ pyrochlore phase. A conventional direct mixing process is not suitable for the preparation of the $PFW_xPFN_{0.9-x}PT_{0.1}$ system.

For complex perovskite relaxors, it has been reported that perovskite is not formed directly from the constituent oxides but from its intermediate phase [5]. In our previous study of double-calcined PFN [6], it was found that nucleation of PFN was accelerated with the formation of $Pb_2Fe_2O_5$. From the above point of view, it was thought that perovskite might also be prepared from the intermediate phase, with a double calcination process, for the system $PFW_xPFN_{0.9-x}PT_{0.1}$.

TABLE II Perovskite phase concentrations of Nos 1 to 7 before and after sintering

Conditions		Perovskite concentration (%)	
		1st/2nd calcination, before sintering	After sintering at 930° C
Case 1	No. 1	28	99
	No. 2	78	99
	No. 3	84	99
	No. 4	86	99
	No. 5	98	99
Case 2	No. 6	100	100
Case 3	No. 7	20	20

3.2. Principle of double calcination process

The concentrations of the perovskite phase before and after the sintering process are listed in Table II. For No. 1 calcining condition, only 28% perovskite phase was obtained. On increasing the second the calcining temperature from 700 to 800° C, the perovskite phase concentration changes from 78 to 98%. After sintering at 930° C, there was no definite difference in the perovskite phase concentrations among Nos 1, 2, 3, 4 and 5. Perovskite phase concentrations of at least 99% were easily synthesized. It is interesting to note that almost all the intermediate phases have been transformed into the perovskite phase in spite of the amounts of intermediate phase present. These intermediate phases do not obstruct the formation of perovskite phase.

Comparing with the result of a conventional ceramic process (discussed in Section 3.1), it can be concluded

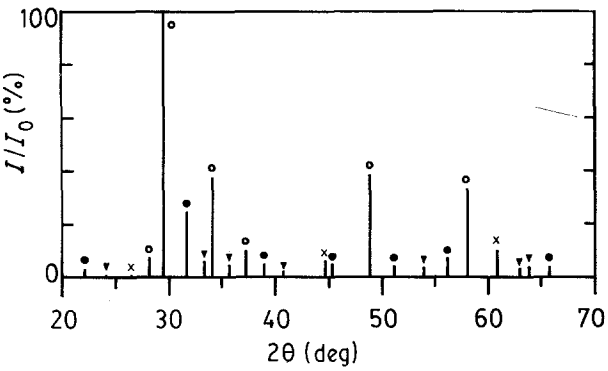

Figure 1 X-ray diffraction pattern of $PFW_{0.41}PFN_{0.49}PT_{0.1}$ fired at 970° C; (●) perovskite, (▼) Fe_2O_3, (○) $Pb_3Nb_4O_{13}$ and (x) undetermined compositions.

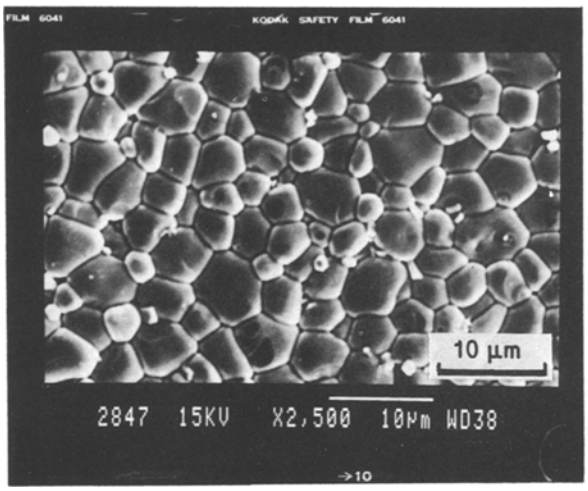

Figure 2 Free surface examination of Specimen No. 2 fired at 900° C.

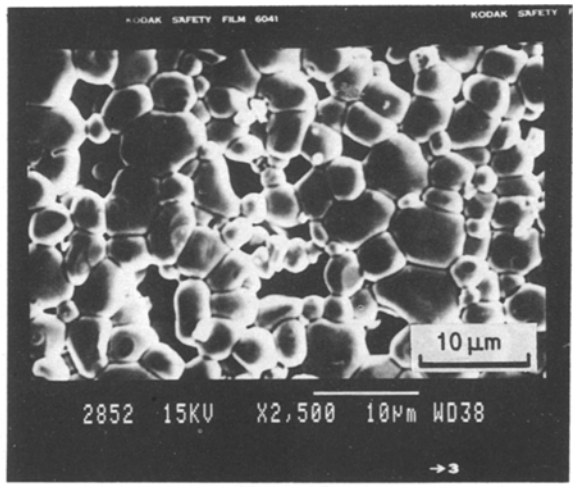

Figure 3 Porous microstructure of Specimen No. 1 fired at 900° C.

that the nucleation of perovskite was taking place via the reaction of the intermediate phase. This demonstrates a remarkable improvement over the conventional ceramic process. The principle of the double calcination process is to transform the raw material into an intermediate phase via the first calcination and then to nucleate perovskite during the second calcination process. If there were considerable amounts of raw material left after the first calcination, the following second calcination would be of no use since such a case is similar to the conventional direct mixing process.

3.3. Effect of processing temperature on the sinterability of $PFW_xPFN_{0.9-x}PT_{0.1}$ (x = 0.41 used for illustration)

In Table III the linear shrinkage and theoretical density are listed as functions of the processing temperature. Two trends in the data presented in Table III are observed. In general the theoretical density and linear shrinkage increase with sintering temperature, but increase first and then decrease when the second calcining temperature exceeded 700° C. Case 1 gave a higher theoretical density and linear shrinkage than Case 2. Comparing the data listed in Tables I and III, one can see that specimens with a higher perovskite phase concentration did not shrink more to become denser bodies. A parasitic intermediate phase did not obstruct the sintering of $PFW_xPFN_{0.9-x}PT_{0.1}$.

Sintering in the presence of an intermediate phase may be similar to that of reaction sintering. Case 2 had a larger grain size than Case 1, as can be seen in Table III. Intermediate phases inhibit and unify the grain size. Examination of the microstructure of No. 2 specimens fired at 930° C, which is shown in Fig. 2, illustrates that a highly dense microstructure is presented. On the other hand, segregation of second phase was scarcely visible along the grain boundaries. This confirms the result deduced from XRD that the intermediate phase was transformed into perovskite and was beneficial to the sinterability.

3.4. Effect of processing temperature on the dielectric properties of $PFW_xPFN_{0.9-x}PT_{0.1}$ (x = 0.41 used for illustration)

The processing temperature dependences of typical dielectric properties of $PFW_{0.41}PFN_{0.49}PT_{0.1}$ are listed in Table IV. It is obvious from the data presented in Tables I and IV that the optimal second calcining temperature and sintering temperature are 700 and 930° C, respectively. In addition, in Cases 1 and 2 the processing temperature showed a significant effect on the Curie temperature. Remarkable differences of Curie temperature existed in specimens prepared from the calcining conditions of Cases 1 and 2.

The degradation of dielectric properties, i.e. higher loss tangent and lower dielectric constant, for samples prepared with a lower second calcining temperature (e.g. No. 1) can be understood from its porous microstructure, as shown in Fig. 3. The porous microstructure was believed to result from the existence of too much intermediate phase after the second calcination.

Typical plots of dielectric constant, loss tangent and variation of capacitance against temperature of samples prepared with different calcining conditions are shown in Figs 4, 5 and 6, respectively. As can

TABLE III Effect of processing temperature on the sinterability of $PFW_{0.41}PFN_{0.49}PT_{0.1}$

Sample No.	Theoretical density (%)			Linear shrinkage (%)			Grain size (µm)		
	900° C	930° C	950° C	900° C	930° C	950° C	900° C	930° C	950° C
1	77.1	83.3	85.4	11.9	12.5	16.5	3.2	3.7	4.1
2	87.7	95.3	93.2	15.8	15.8	15.8	3.8	4.2	4.5
3	87.3	92.5	90.8	14.8	15.7	15.2	3.8	5.8	6.5
4	85.6	91.9	91.0	13.9	15.7	15.4	4.0	6.0	5.7
5	84.2	91.0	90.9	11.7	13.9	14.5	4.1	6.3	6.1
6	77.1	83.3	86.4	10.1	12.8	13.9	4.3	6.8	7.8

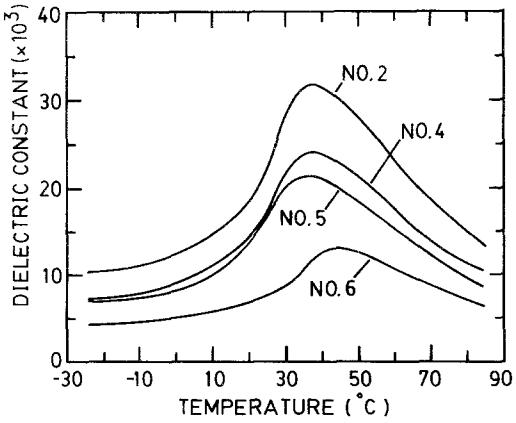

Figure 4 Temperature dependences of dielectric constant, with different calcining conditions, for $PFW_{0.41}PFN_{0.49}PT_{0.1}$ fired at 930° C.

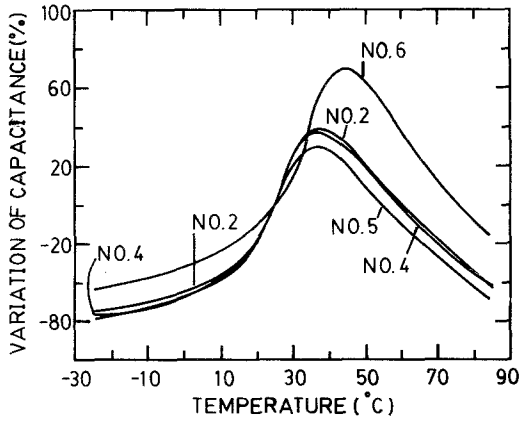

Figure 6 Temperature dependences of percentage variation of capacitance, with different calcining conditions, for $PFW_{0.41}PFN_{0.49}PT_{0.1}$ fired at 930° C.

be seen in Figs 4 and 5, the dielectric constant–temperature curve was shifted upward, while the curve of loss tangent against temperature was depressed by decrease of the second calcining temperature. Apparently, 700° C is a better second calcining temperature. However, the variations of capacitance were all outside the Z5U specifications of +22% to −56%, even when the x value of $PFW_xPFN_{0.9-x}PT_{0.1}$ was changed. To make the system meet the requirements of Z5U dielectrics, addition of depressor is necessitated.

Fig. 7 shows the dependence of dielectric constant on sintering temperature. The curve of dielectric constant against temperature was shifted upward with increasing sintering temperature up to 930° C and then downward for temperatures higher than 930° C. Referring to the data of Table III, the grain size increased with either sintering temperature or second calcining temperature. Swartz *et al.* [7] ascribed increases of room-temperature dielectric constant and maximum dielectric constant with grain size to a decrease of the low dielectric constant (LoK) phase at grain boundaries, but the cases of Figs 4 and 7 behaved in a different way. In Fig. 7 the dielectric constant increased and then decreased with the grain size when the sintering temperature was increased. If the increase in grain size was attributable to the increase of the second calcining temperature, the dielectric constant would decrease with the grain size (as is the case of Fig. 4). From the above discussion it is difficult to state whether the change of dielectric constant is dependent on grain size or not. It is clear from Table III that the optimum bulk density was achieved with a lower calcining temperature of 700° C and an intermediate firing temperature of 930° C (compared with other sintering temperatures in this work). The increase of dielectric constant in both Figs 4 and 7 may result from the higher bulk density. The decrease of dielectric constant above the optimum processing temperature was due to grain growth and the appearance of LoK granular pores, as can be seen in Fig. 8.

3.5. Frequency dependence of dielectric properties

The temperature dependences of dielectric constant and loss tangent of $PFW_{0.41}PFN_{0.49}PT_{0.1}$ at both 1 and 100 kHz are illustrated in Fig. 9. A degradation of the relaxing properties was found. The value of the maximum loss tangent below the Curie temperature was only 2%, while the typical value for a relaxor is approximately 10%. The transition range did not shift definitely to higher temperatures when the measuring frequency changed from 1 to 100 kHz. Degradation of the relaxation properties was caused by the sharper phase transitions of PFN and PT.

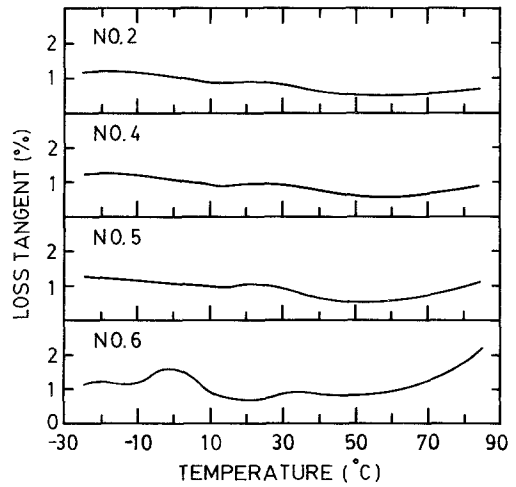

Figure 5 Temperature dependences of loss tangent, with different calcining conditions, for $PFW_{0.41}PFN_{0.49}PT_{0.1}$ fired at 930° C.

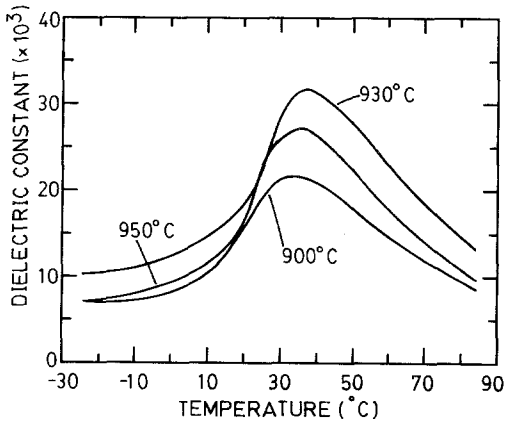

Figure 7 Temperature dependences of the dielectric constant of specimen No. 2 with different sintering temperatures.

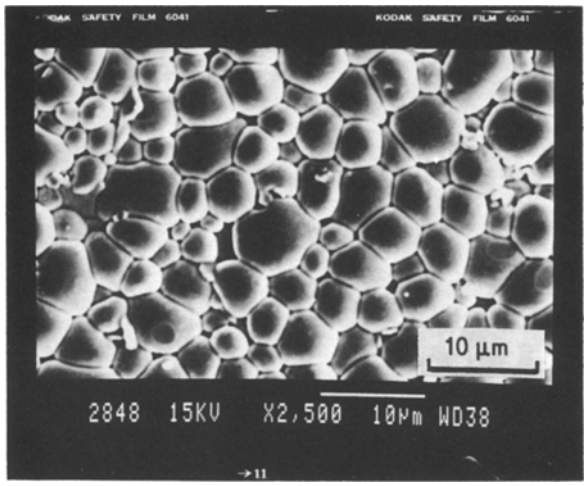

Figure 8 Free surface examination of Specimen No. 2 fired at 950° C.

4. Conclusions

A double calcination process was developed to prepare at least 99% perovskite solid solution. The double calcination process is based on the fact that perovskite can be formed from its intermediate phase, and not from the constituent oxides alone. Suitable amounts of intermediate phase, determined by the second calcination, possess the ability of reaction sintering. This process has a remarkable effect on the improvement of the conventional ceramic process for $PFW_xPFN_{0.9-x}PT_{0.1}$ ceramics.

$PFW_xPFN_{0.9-x}PT_{0.1}$ ceramics could be applied as low-firing Z5U dielectrics for MLC if the capacitance–temperature characteristics were improved.

Further work will involve the study of the formation mechanism of $PFW_xPFN_{0.9-x}PT_{0.1}$ prepared by the double calcination process and the dielectric applications of such ceramics.

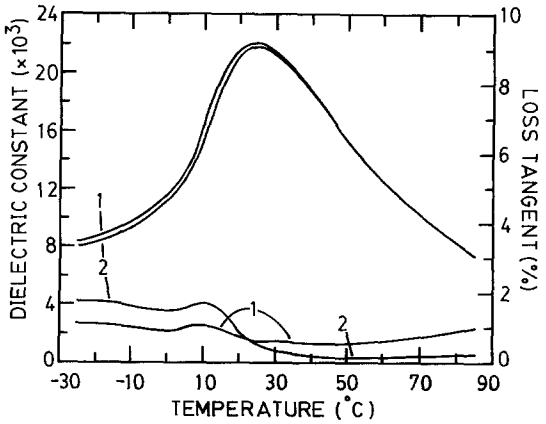

Figure 9 Frequency dependences of dielectric properties of $PFW_{0.41}PFN_{0.49}PT_{0.1}$ ceramics sintered at 930° C: (1) 1 kHz, (2) 100 kHz.

Acknowledgements

The authors wish to express their gratitude to the National Science Council of the Republic of China for their financial support on this study.

References

1. T. R. SHROUT and A. HALLIYAL, *Bull. Amer. Ceram. Soc.* **66** (1987) 704.
2. S. L. SWARTZ and T. R. SHROUT, *Mater. Res. Bull.* **17** (1982) 1245.
3. M. LEJEUNE and J. P. BOILOT, *ibid.* **20** (1985) 493.
4. E. M. LEVIN, C. R. ROBBINS and H. F. McMURDIE, in "Phase Diagrams for Ceramist", edited by M. K. Reser (American Ceramic Society, Columbus, Ohio, 1964) p. 117 (Fig. 325).
5. M. P. KASSARJIAN, R. E. NEWNHAM and J. M. BIGGERS, *Bull. Amer. Ceram. Soc.* **64** (1985) 1108.
6. S. L. FU and G. F. CHEN, *Ferroelectrics* (1988) in press.
7. S. L. SWARTZ, T. R. SHROUT, W. A. SCHULZE and L. E. CROSS, *J. Amer. Ceram. Soc.* **67** (1984) 311.

Received 15 September 1987
and accepted 19 January 1988

TABLE IV Effect of processing temperature on the dielectric properties of $PFW_{0.41}PFN_{0.49}PT_{0.1}$

Sample No.	Dielectric constant			Loss tangent (%)			Curie temperature		
	900° C	930° C	950° C	900° C	930° C	950° C	900° C	930° C	950° C
1	13870	17300	14450	5.67	4.4	2.58	–	–	–
2	19050	22850	23000	0.97	0.97	0.71	34	37	36
3	17380	20160	21370	1.18	0.9	0.65	34	37	38
4	15330	17460	17690	3.17	1.1	1.01	34	37	39
5	13460	16800	17920	1.12	1.3	0.75	33	37	39
6	5400	7620	7630	0.9	0.9	1.25	40	45	49